arXiv:1611.00513v2 [astro-ph.HE] 25 Nov 2016

Radiative shock waves and their role in solving puzzles of Superluminous Supernovae

S.I. Blinnikov[1,2]

[1]ITEP, 117218, Moscow, Russia, Sergei.Blinnikov@itep.ru
[2]Kavli IPMU (WPI), The University of Tokyo, Kashiwa, 277-8583, Japan

1 Introduction: Three paths, i.e. three scenarios proposed for SLSNe

Typical supernova (or SN) explosions produce ejecta with kinetic energies 10^{51} ergs $\equiv 1$ foe. This unit of energy was introduced by H.Bethe and is an abbreviation of 10 to **fifty one ergs**. Light emitted during the first year of supernova is only a small fraction, around 0.01 foe. Many supernovae are discovered in last decade with peak luminosity one-two orders of magnitude higher than for normal supernovae of known types. They emit powerful light with energy approaching 1 foe, and sometimes even higher.

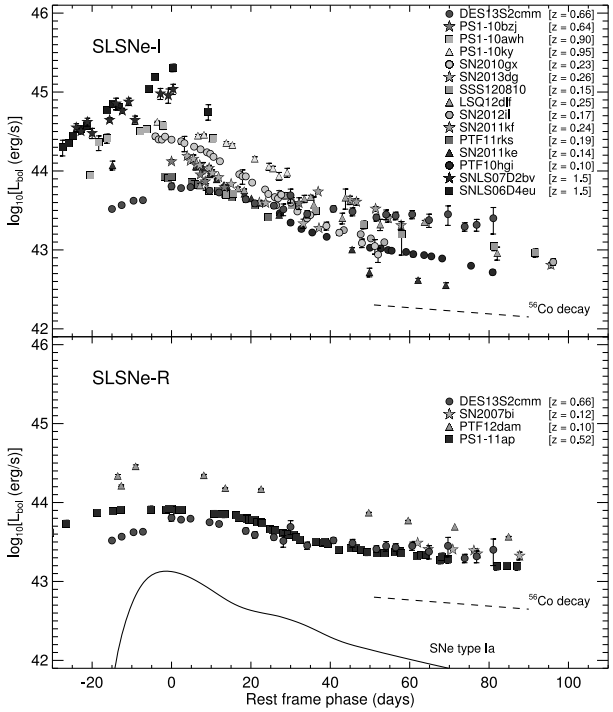

Fig. 1: Bolometric light curves of some Superluminous Supernovae. From paper [1]

An example is given in Figure 1 together with a typical SN Ia (used for cosmology due to their high luminosity) for comparison. We see that the new objects emit much more light. They are called Superluminous supernovae: SLSNe. This is a challenge for theory, since even normal supernovae are not yet completely understood from the first principles.

Many models are discussed in literature on SLSNe, but it seems that the most viable are the following three scenarios.

1. Pair Instability Supernovae, **PISN**
2. **"Magnetar"** pumping (taking in quotes, since observed magnetars are slowly rotating in Soft Gamma-ray Repeators, and here millisecond periods are needed)
3. **Shock** interaction with Circumstellar Matter (CSM), e.g. Pulsational pair instability, **PPISN**

2 Pair Instability and Supernovae

To understand the mechanism of explosion of Pair Instability Supernovae one has to learn a bit on stellar evolution theory.

Figure 2 shows the evolutionary tracks of normal stars of various masses.

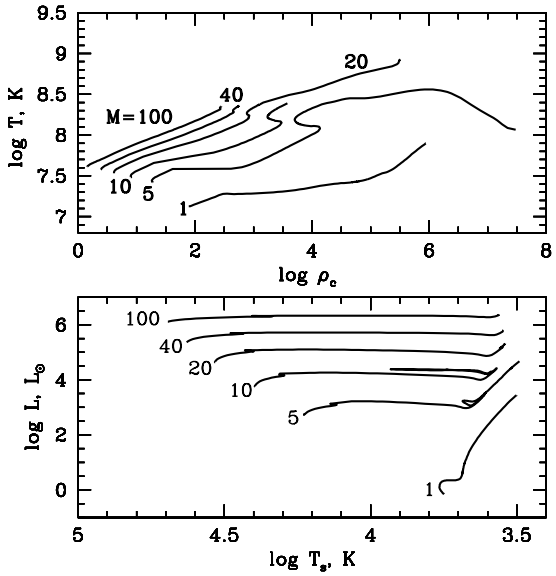

Fig. 2: Evolution of central temperature vs. central density (upper panel) and Hertzprung-Russel diagram (lower panel) for a few models of normal stars. Numbers near the tracks are masses of stars in units of solar mass $M_\odot$

One can easily notice a trend: central temperature T_c grows with central density ρ_c approximately as $T_c \propto \rho_c^{1/3}$. This law is more pronounced for more massive stars. This relation is easily understood from the conditions of mechanical equilibrium of a star.

A very crude order-of-magnitude estimate for the attraction force of two halves of a star with mass M is

$$F \sim \frac{G_{\rm N} M^2}{4R^2},$$

where R is the star radius, and $G_{\rm N}$ is the Newton's constant. This force must be balanced by a gradient of pressure P in a star which is in equilibrum.

Pressure P is virtually zero on the surface, and in the center

$$P_c = \frac{F}{S} = \frac{F}{\pi R^2}.$$

Omitting all coefficients of order unity, we get for the pressure and density in the center:

$$P_c \simeq \frac{G_{\rm N} M^2}{R^4},$$

$$\rho_c \simeq \frac{M}{R^3},$$

and we find that the equilibrium requires (in **Newtonian gravity**):

$$P_c \simeq G_{\rm N} M^{2/3} \rho_c^{4/3}.$$

So if we have a classical ideal plasma with

$$P = \mathcal{R}\rho T/\mu,$$

where $\mathcal{R}$ is the universal gas constant, and μ is mean molecular mass, we get for the central temperature

$$T_c \simeq \frac{G_{\rm N} M^{2/3} \rho_c^{1/3} \mu}{\mathcal{R}}.$$

Thus, $T_c \propto M^{2/3} \rho_c^{1/3}$ in non-degenerate stars and for a given mass

$$T_c \propto \rho_c^{1/3}$$

The same 1/3 power is obtained for radiation-dominated massive stars (but with $M^{1/6}$).

The condition of mechanical equilibrium,

$$P_c \simeq G_{\rm N} M^{2/3} \rho_c^{4/3},$$

tells us quickly something on hydrodynamical stability of a star. It implies that adiabatic exponent $\gamma < 4/3$ may lead to a hydrodynamical instability. Indeed, if $\gamma < 4/3$ then a global compression of the star produces physical pressure which is **lower** than needed for the equilibrium. Then gravity wins over pressure and the star starts collapsing.

Relativistic particles, i.e. photons lead to $\gamma \to 4/3$. In massive stars, with $M \sim 100 M_\odot$ we have $\gamma \sim 4/3$ due to high entropy S (we have many photons per baryon).

A radiation dominated massive star was already at the verge of the loss of the stability, pressure was close to the law ($P \propto \rho^{4/3}$), and now it loses it: γ becomes less than 4/3 since the creation of e^+e^- pairs requires energy. The momenta of particles at compression do not grow fast enough: the pairs are created with particles having low speed. The loss of mechanical stability at $\rho_c \sim 10^4$ gcc leads to the beginning of gravitational collapse which may be halted at $\rho_c < 10^7$ gcc by a powerful explosion, if the star has enough nuclear fuel (mostly oxygen) in the centre. The explosion gives kinetic energy up to about 70 foe, and enough light to explain some of SLSNe due to production of huge amount of radioactive ^{56}Ni: up to $\sim 20 M_\odot$ (while in standard thermonuclear supernovae this amount is 20 - 50 times smaller).

This model, which is called PISN (Pair Instability Supernova), is able to explain some of SLSN events but only the slow ones, due to the long diffusion time of photons in ejecta overwhelmed by the iron peak elements (products of the explosion itself and of ^{56}Ni decay).

Similar slow light curves are produced by "Magnetar" pumping. There are many uncertainties in the magnetar model, which also involves huge energy of tens foe extracted from rotational energy of a neutron star. I do not discuss it here, and go directly to the most economical model which is especially good for fast SLSNe.

3 Models with radiating shock waves

The models explaining SLSN events with the minimum energy budget involve multiple ejections of mass in presupernova stars. The radiative shocks produced in collisions of those shells may provide the required power of light. This class of the models is referred to as "interacting" supernovae. Nonlinear effects are important on all stages of the superluminous supernova phenomenon: from the initial mass ejections, then at the maximum light and through the supernova remnant with fragmentation of dense shells.

Let us obtain some estimated for important quantities.

Luminosity is expressed through effective temperature $T_{\rm eff}$ and photospheric radius $R_{\rm ph}$:

$$L = 4\pi\sigma T_{\rm eff}^4 R_{\rm ph}^2 \qquad (1)$$

for the age of supernova $t = 10$ d and typical velocity at the photosphere level $u = 10^9$ cm/s (i.e. 10 thousand km/s) we get $R_{\rm ph} = ut \approx 10^{15}$ cm, and if a typical $T_{\rm eff} \sim 10^4$ K, then $L \sim 10^{43}$ erg/s.

Luminosity L goes down in some weeks, thus, ordinary, non-interacting supernovae produce $\sim 10^{49}$ ergs= 0.01 foe in photons during the first year after explosion, while $\sim 10^{51}$ ergs= 1 foe remain in the kinetic energy of ejecta in "standard" SN explosions.

This energy is radiated much later, during millennia after the explosion (mostly in X-rays) by the supernova remnant in the shocks produced by ejecta in ordinary interstellar medium with the number density ~ 1 cm^{-3}. If the density of CSM is billion times higher, then a large fraction of the kinetic energy will be radiated away much faster, on a time scale of a year and the photons will be much softer than X-ray, they will be emitted mostly in visible or ultraviolet range.

We may have the same typical $T_{\rm eff} \sim 10^4$ K, while $R_{\rm ph} \sim 10^{16}$ cm is much larger and the luminosity goes up approaching $L \sim 10^{45}$ erg/s for some period of time. Thus a superluminous supernova (SLSN) can be produced for the energy of explosion on the standard scale of 1 foe $\sim 10^{51}$ ergs, but now a major fraction of this energy is lost during the first year.

If we have a blob of matter with mass m_1 and momentum $\mathbf{p_1}$ its kinetic energy is

$$E_1 = \frac{\mathbf{p_1}^2}{2m_1}. \tag{2}$$

If it is colliding with another blob with mass m_0 and zero momentum we get for the final energy of two merged blobs in a fully inelastic collision

$$E_2 = \frac{\mathbf{p_1}^2}{2(m_1+m_0)}. \tag{3}$$

The momentum is conserved, but the energy in amount $E_1 - E_2$ is radiated away, since $E_2 < E_1$. If $m_0 \ll m_1$ only a tiny fraction of E_1 is radiated, but if $m_0 \gg m_1$, then $E_2 \ll E_1$ and almost all initial E_1 is radiated away.

This means that collisions of low mass and fast moving ejecta with heavy (dense) slowly moving blobs of CSM are efficient in producing many photons. Of course one should remember that in this case the momentum of the two merged blobs may be different from the initial $\mathbf{p_1}$ if we have a directed flux of newborn photons which carry some net momentum away.

There is no much sense in evaluating this effect using the order-of-magnitude estimates because the details of the production of photons may be complicated. The degree of "inelasticity" of the collision depend on the pattern of hydrodynamic flow and on the properties of emission/absorption of the plasma, e.g. on its composition. Anyway, those details and conservation of momenta and energy must be taken into account in full radiation hydrodynamic simulations.

Now let us find the temperature behind the shock front. Again on the level of simple estimates for the pressure behind the shock front P_s we have

$$P_s \sim \rho_0 D^2 = n_0 m_i D^2 \tag{4}$$

if the density upstream the front is ρ_0, and D is the velocity of the front. The density $\rho = n m_i$ with n number density and m_i averaged mass of ions. The estimate (4) follows from the momentum conservation: the momentum flux is $P + \rho u^2$ for the flow having velocity u, and P is negligible ahead of the front where the matter is cold. More accurate expression for P_s is easily derived from the laws of conservation.

The estimate (4) gives for a non-relativistic plasma with pressure $P = nk_BT$:

$$k_B T_s \sim m_i D^2 \tag{5}$$

which suggests very high temperatures, in keV range and higher for shock velocities larger that a thousand km/s.

Now I will derive "exact" coefficients in (5).

Let us use standard notations for density ρ, velocity u, pressure P, thermodynamic energy E, and define

$$U_1 = \rho,$$

density of momentum

$$U_2 = \rho u,$$

total energy density

$$U_3 = E + \frac{\rho u^2}{2}.$$

We also define fluxes of mass, $F_1 = \rho u$,
of momentum, $F_2 = \rho u^2 + P$,
and of energy $F_3 = (E + \rho u^2/2 + P)u$, and we have a general law of conservation:

$$\frac{\partial \vec{U}}{\partial t} = -\frac{\partial \vec{F}}{\partial x}.$$

In a stationary case, i.e. $\partial \vec{U}/\partial t = 0$, we get $\vec{F} = \text{const}$. Introduce

$$j \equiv \rho u = \text{const}, \qquad V \equiv \frac{1}{\rho}\ .$$

From $F_2 = \rho u^2 + P = j^2 V = \text{const}$ we obtain:

$$j^2 V_0 + P_0 = j^2 V_s + P_s \to P_s = P_0 + j^2 (V_0 - V_s)\ ,$$

Subsript "0" for ρ, V, u, P, E denotes the initial values upstream (ahead of the shock front), while "s" corresponds to the values downstream, in the shocked matter. It is most convenient to work in the reference frame where the front is at rest, then the speed of the shock D is just u_0, because by definition it is measured relative the unshocked matter.

Now $F_3 = \text{const}$ gives:

$$(E_0 + \tfrac{1}{2} j^2 V_0 + P_0) u_0 = (E_s + \tfrac{1}{2} j^2 V_s + P_s) u_s$$

If we replace here $u_i \to j V_i$, we get:

$$(E_0 + \tfrac{1}{2} j^2 V_0 + P_0) j V_0 = (E_s + \tfrac{1}{2} j^2 V_s + P_s) j V_s\ .$$

From here

$$E_0V_0 + \tfrac{1}{2}j^2V_0^2 + P_0V_0 = E_sV_s + \tfrac{1}{2}j^2V_s^2 + P_sV_s \ ,$$

and

$$(E_0 + P_0)V_0 + \tfrac{1}{2}j^2(V_0^2 - V_s^2) = (E_s + P_s)V_s \ .$$

But $(V_0^2 - V_s^2) = (V_0 - V_s)(V_0 + V_s)$ and $P_s = P_0 + j^2(V_0 - V_s)$ obtained above implies $V_0 - V_s = (P_s - P_0)/j^2$, so j^2 cancels in numerator and denominator:

$$(E_0 + P_0)V_0 + \tfrac{1}{2}\cancel{j^2}\frac{(P_s - P_0)}{\cancel{j^2}}(V_0 + V_s) = (E_s + P_s)V_s \ .$$

Thus,

$$\left(E_0 + \frac{P_0 + P_s}{2}\right)V_0 = \left(E_s + \frac{P_0 + P_s}{2}\right)V_s \ ,$$

and we obtain a general formula for the compression in the flow (e.g. on a shock front):

$$\frac{V_s}{V_0} = \frac{2E_0 + P_0 + P_s}{2E_s + P_0 + P_s} \ .$$

An equation of state $E = E(P, V)$, or $P = P(E, V)$ gives the shock adiabat. For a general equation of state in a strong shock ($P_s \gg P_0$, $E_s \gg E_0$) which is most important in supernova envelopes,

$$\frac{V_s}{V_0} = \frac{2E_0/(P_0 + P_s) + 1}{2E_s/(P_0 + P_s) + 1} \approx \frac{1}{2E_s/P_s + 1} \ ,$$

or

$$\frac{\rho_s}{\rho_0} = \frac{V_0}{V_s} \approx 1 + \frac{2E_s}{P_s} \ ,$$

in general case, and

$$\frac{\rho_s}{\rho_0} = \frac{V_0}{V_s} \approx 1 + \frac{2}{\gamma - 1} = \frac{\gamma + 1}{\gamma - 1} \ ,$$

for the case of $\gamma = \text{const}$ equation of state.

Let $P = (\gamma - 1)E_{\rm tr}$, where $E_{\rm tr}$ is translational internal energy, i.e. kinetic energy of particles in plasma, and let $E = E_{\rm tr} + Q$, where Q is, e.g., ionization potential energy. Then in a strong shock

$$\frac{\rho_s}{\rho_0} = \frac{V_0}{V_s} \approx 1 + \frac{2E_{2\rm tr} + 2Q}{P_s} = 1 + \frac{2}{\gamma - 1} + \frac{2Q}{(\gamma - 1)E_{2\rm tr}} \ ,$$

that is

$$\frac{\rho_s}{\rho_0} = \frac{V_0}{V_s} \approx \frac{\gamma + 1}{\gamma - 1} + \frac{2Q}{(\gamma - 1)E_{2\rm tr}} \ .$$

For $\gamma = 5/3$ this gives

$$\frac{\rho_s}{\rho_0} = \frac{V_0}{V_s} \approx 4 + \frac{3Q}{E_{2\rm tr}} \ ,$$

— formula (3.71) in the famous book on shocks written by Zeldovich and Raizer.

We found from conservation of momentum ($F_2 = \text{const}$) that $P_s = P_0 + j^2(V_0 - V_s)$, i.e.

$$j^2 = \frac{P_s - P_0}{V_0 - V_s} \approx \frac{P_s}{V_0 - V_s} = \frac{P_s}{V_0[1 - (\gamma - 1)/(\gamma + 1)]} = \frac{P_s(\gamma + 1)}{2V_0} \ ,$$

— this is valid for a strong shock, constant γ and small Q. Hence,

$$\rho_0^2 u_0^2 = \frac{P_s(\gamma + 1)\rho_0}{2} \ ,$$

that is

$$P_s = \frac{2}{\gamma + 1}\rho_0 u_0^2. \tag{6}$$

Note that γ here must be taken for the gas behind the strong shock since the pressure P_0 is negligible and its equation of state is irrelevant.

For a non-relativistic plasma with pressure $P = \mathcal{R}\rho T/\mu$ we get from (6)

$$\rho_0 u_0^2 = \frac{(\gamma + 1)\mathcal{R}\rho_s T_s}{2\mu} \ ,$$

so

$$u_0^2 = \frac{(\gamma + 1)\mathcal{R}\rho_s T_s}{2\rho_0\mu} = \frac{(\gamma + 1)^2\mathcal{R}T_s}{2(\gamma - 1)\mu} \ .$$

The postshock temperature T_s for the strong shock, constant γ and small Q is (from the last equation)

$$T_s = \frac{2(\gamma - 1)u_0^2\mu}{(\gamma + 1)^2\mathcal{R}} \ .$$

For $\gamma = 5/3$ we get

$$T_s = \frac{3u_0^2\mu}{16\mathcal{R}} \ . \tag{7}$$

If we put here $D_8 = u_0/10^8\text{cm/s}$, then D_8 is the shock speed in thousand km/s and we get

$$T_s(\text{K}) = 2.25 \times 10^7 \mu D_8^2 \tag{8}$$

in Kelvins or

$$T_s(\text{keV}) = 1.94\mu D_8^2 \tag{9}$$

in keV. Here $\mu = A/(1+Z)$ for plasma (since $n = n_{\rm baryon}/\mu = n_{\rm ion}A/\mu = n_{\rm ion} + n_e = n_{\rm ion} + Zn_{\rm ion}$). Note that a typical value for D in SNe is about 10 thousand km/s, so T will be of order 10^9 K or hundreds keV.

Since $\mathcal{R} \approx k_B/m_p$ where m_p is proton mass, we have

$$k_B T_s \sim m_p D_s^2. \tag{10}$$

This estimate is the same as used in Eq.(5) if we put $m_i = m_p$.

In supernova envelopes these numbers are misleading!

In reality plasma in supernova conditions is at least partly relativistic: we have a huge number of photons with $P = aT^4/3$, and so T_s is appreciably lower due to high heat capacity of photon gas. See Equations (12, 13) below, they show that, with account of radiation for D of order of a thousand km/s and for $\rho \sim 10^{-12}$ gcc, we have $T_s = 4.3 \times 10^4$ K, well below X-ray range of temperatures, but high enough to support high L for a long time at large R.

Using $\gamma = {\rm const}$ is a favourite approximation in many papers and simulations in astrophysics, but in supernovae it is a very bad one, and almost irrelevant. The value of γ varies due to ionization/excitation of atoms, and changes strongly on the shock front when it goes through the cold layers and heats the plasma so strongly that radiation pressure dominates downstream behind the front. In that case (which is quite general for supernova shock breakout) the formulas (8,9) are not applicable and misleading. The equations for mass, momentum and energy conservation are more complicated for radiative shock waves, when one has to account for the transfer of momentum and energy of photons. Nevertheless, there are two important limiting cases for strong shocks with radiation when simple expressions can be derived.

In the first case we may have relatively cold gas upstream with $P_0 \ll P_s$ in the strong shock, and the gas downstream is opaque with the pressure dominated by radiation.

Due to a high heat capacity of photon gas, the temperature behind the front is orders of magnitude lower than in (8),(9).

Let us put radiation pressure for P_s into (6), we get

$$\frac{aT_s^4}{3} = \frac{2}{\gamma+1}\rho_0 u_0^2. \tag{11}$$

We have $\gamma = 4/3$ for the radiation dominated gas, and, substituting $u_0 = D$, we obtain

$$T_s = \left(\frac{18}{7a}\rho_0 D^2\right)^{1/4}. \tag{12}$$

That is

$$T_s(K) = 4.3 \times 10^4 \rho_{-12}^{1/4} D_8^{1/2}, \tag{13}$$

if we normalize density for $\rho = 10^{-12}$ gcc and take D in units of thousand km/s. The temperature in reality is much less than in (8).

The second important case takes place when the radiation is not trapped, its pressure and momentum may be neglected, but when it is very efficient in heat transport. Now the energy is not conserved, and the energy flux F_3 is not constant any more. Instead of this we may have the constancy of temperature ahead and behind the front. Mass and momentum conservation give as before:

$$P_s = P_0 + j^2(V_0 - V_s). \tag{14}$$

Now both upstream and downstream, the pressure is $P = \mathcal{R}\rho T/\mu$ with the same T, so the strong shock condition, $P_s \gg P_0$ means not a high T behind the front, but $\rho_s \gg \rho_0$, and $P_s \approx \rho_0 u_0^2$, which we get from (14), gives

$$\frac{\rho_s}{\rho_0} = \frac{\mu D^2}{\mathcal{R}T}. \tag{15}$$

The isothermal T here is much less than the temperature found in (8),(9) for adiabatic shocks, hence the compression in isothermal shocks may be orders of magnitude larger than the canonical $(\gamma+1)/(\gamma-1)$ of adiabatic shocks. This is a typical situation for formation of cool dense shells in interacting supernovae. The exact value of T and of the compression depends on the details of the properties of plasma with respect to heat conduction, but one should remember that those dense shells may become unstable, and the exact numbers found in idealized accurate plane parallel or spherically symmetric calculations may be not very useful.

4 Numerical simulations of light curves

I describe some results of numerical simulations which take into account radiation trapping effects in interacting supernovae. For illustration I use the results from paper [2].

The simulations use presupernovae structures obtained either from evolutionary codes or artificially constructed. Anyway, the initial models have a fast moving part which may be called "ejecta". This part has mass $M_{\rm ej}$ and radius $R_{\rm ej}$. $M_{\rm ej}$ can be much less than the total mass of the collapsing core; it is just a convenient form of parametrization of models.

To make an interacting model the ejecta are surrounded by a rather dense envelope, "wind", with the mass $M_{\rm w}$ extended to the radius $R_{\rm w}$. The outer radius of this envelope must be large $\sim 10^{16}$ cm or even larger for extreme cases. The envelope may have a power-law density distribution $\rho \propto r^{-p}$, which simulates the wind that surrounds the exploding star. For a steady wind, $p = 2$, but in the very last stages of the evolution of a presupernova star the wind may not be steady and the parameter p may be varied in the range between 1.5 and 3.5. Another kind of envelope, detached from the ejecta by a region of lower density, is also considered in our simulations.

The light curves are calculated for SNe exploding within these envelopes. A shock wave forms at the border between the ejecta and the envelope. The shock very efficiently converts the energy of the ordered motion of

expanding gas to that of the chaotic thermal motion of particles, which can be easily emitted. As a result, one may expect to obtain light curves powerful enough to explain at least a part of superluminous SNe without an assumption of unusually high explosion energy. The detailed computations support those expectations.

For type IIn SLSNe, that is narrow-line events, hydrogen rich envelopes are used. For SLSN I (no hydrogen in spectra) carbon-oxygen models with different C to O ratios or helium models are typically employed. The models may contain some amount of radioactive elements like ^{56}Ni, but it is not necessary in this class of simulations since the effect of pure ejecta-CSM interaction is sufficient for explaining majority of SLSNe with zero amount of ^{56}Ni.

The synthetic light curves in [2] are calculated using our multi-group radiation hydrodynamic code STELLA in its standard setup. The code simulates spherically symmetric hydrodynamic flows coupled with multi-group radiative transfer. The opacity routine takes into account electron scattering, free-free and bound-free processes. Contribution of spectral lines (i.e. bound-bound processes) is treated in approximation of "expansion" opacity.

The explosions have been simulated as a "thermal bomb" with variable energy $E_{\rm expl}$ of the order 2 - 4 foe (1 foe = 10^{51} ergs), which is a bit larger than in a standard 1 foe supernova, but much lower than invoked in hypernovae or in PISNe (pair-instability supernovae).

Figure 3 shows how the profiles of density, velocity, temperature, and Rosseland mean optical depth evolve along time for one of the models. The left panels correspond to the evolution before maximum of the light curve (which happens on day 27 after the explosion for that model) the right panels show the evolution after maximum.

At the very beginning, the shock wave structure starts to form due to collision between the ejecta and the CSM. Then the emission from the shock front heats the gas in the envelope, thus making it opaque, and the photosphere moves to the outermost layers rather quickly. When the photospheric radius reaches its maximum, one can observe maximal emission from the supernova.

The speed of the growth of the photospheric radius depends on the mass of the envelope, since more photons must be emitted from the shock to heat larger mass envelopes.

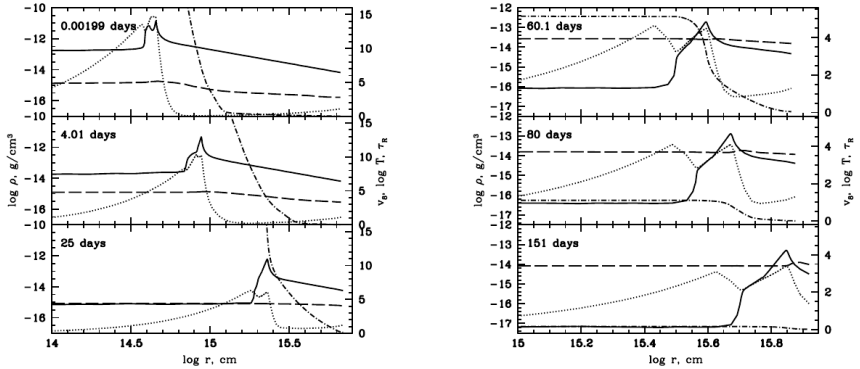

Fig. 3: Evolution of radial profiles of the density (*solid lines*), velocity (in 10^8 cm s^{-1}, *dots*), matter temperature (*dashes*), and Rosseland optical depth (*dash-dots*) for one of the models [2]. The scale for the density is on the left Y axis, for all other quantities, on the right Y axis. Left panel: evolution of the hydrodynamical structure before maximum: very soon after the explosion and at days 4 and 25. Right panel: the same parameters, but after maximum: at days 60, 80, and 151. Note that different scales for the axes are used on the left and right panels.

Another parameter which impacts the initial growth of the photospheric radius is the chemical composition of the envelope. E.g., the light curve rises faster for a CO envelope than for a He one as a lower temperature is needed to reach high opacity in a CO mixture. This light curve behaviour can help set the composition for some observed SLSNe.

The plots on the right-hand side of Figure 3 show the stages when the photosphere slowly moves back to the center, and the envelope and the ejecta finally become fully transparent. At the beginning of this post-maximum stage all gas in the envelope is already heated by the photons which came from the shock region and diffused through the envelope to the outer edge, and the whole system (ejecta and envelope) becomes almost isothermal. The shock becomes weaker with time and emits fewer photons which can heat up the envelope, so the temperature of the still unshocked envelope falls down.

The shocked material is gathered into a thin, dense layer which finally contains almost all mass in the system. Formation of this layer leads to numerical difficulties, which significantly limit the time step of the calculation. Another problem can also take place due to the thin layer formation: a thin, dense shell with a very large radius would most probably be unstable and can fragment into smaller lumps. Then the problem would become essentially multi-dimensional.

On the velocity profiles, the multi-reflection structure forms from the very beginning. It evolves very quickly to the standard two-shock (forward and reverse) picture. This does not depend on the initial velocity profile in

the envelope. The interaction of the ejecta with the envelope leads to similar final velocity structures. It looks like a self-similar behaviour analogous to the solution found by Nadyozhin and Chevalier but with radiation.

Figure 4 demonstrates how the model with hydrodynamic evolution shown in Figure 3 reproduces multi-band observations of the well studied Superluminous SN 2010gx.

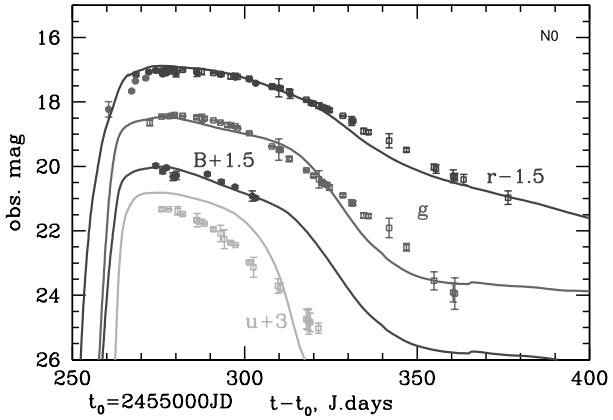

Fig. 4: Synthetic light curves for the model from Fig. 3, one of the best for SN 2010gx, in r, g, B, and u filters compared with Pan-STARRS (u and g bands) and PTF observations (B and r).

Acknowledgements

The work on calculation of the SLSN light curves is supported by a grant of Russian Science Foundation 14-12-00203.

References

1. *Papadopoulos, A.* DES13S2cmm: the first superluminous supernova from the Dark Energy Survey. *A. Papadopoulos, and 68 colleagues.* // Monthly Notices of the Royal Astronomical Society. 2015. V. 449, P. 1215—1227.

2. *Sorokina, E.I.* Type I Superluminous Supernovae as Explosions inside Non-Hydrogen Circumstellar Envelopes. *E.I. Sorokina, S.I. Blinnikov, K. Nomoto, R. Quimby, A. Tolstov.* // The Astrophysical Journal. 2016. V. 829, P. 17.